

Supplementary Information

Shiladitya Karmakar, Soumendu Datta, and Tanusri Saha-Dasgupta*

*Satyendra Nath Bose National Centre for Basic Sciences, Block JD, Sector III, Salt Lake,
Kolkata 700106, India*

E-mail: tanusri@bose.res.in

Content :

Section S1 : Phonon density of states for the pristine TiNI and Janus $\text{Ti}_2\text{N}_2\text{XI}$ (X = Br, Cl) mono-layers

Section S2 : AIMD results at 300 K of the two Janus $\text{Ti}_2\text{N}_2\text{XI}$ mono-layers

Section S3: PDOS of the studied mono-layer from PBE+D3+SOC calculation

Section S4: HSE band-structure of the two Janus mono-layers under strain

Section S1

To confirm the dynamical stability of the two constructed Janus mono-layers, their phonon dispersion were studied. Phonon dispersion was calculated employing finite displacement technique. The dynamical matrix for a displacement of 0.01 \AA , was estimated from the PBE-GGA+D3+SO calculations over a supercell of $5 \times 5 \times 1$ of the unit cell containing total 150 atoms for each Janus mono-layer, using Density Functional Perturbation Theory (DFPT) as implemented in the VASP code. Subsequently, the phonon density of states (DOS) were calculated by PHONOPY interface.¹ During the phonon DOS calculations, $32 \times 32 \times 64$ irreducible q-points sampling mesh and Gauss broadening 0.1 THz were used, which were found to be sufficient to reach the required convergence. The results are shown in Figure 1.

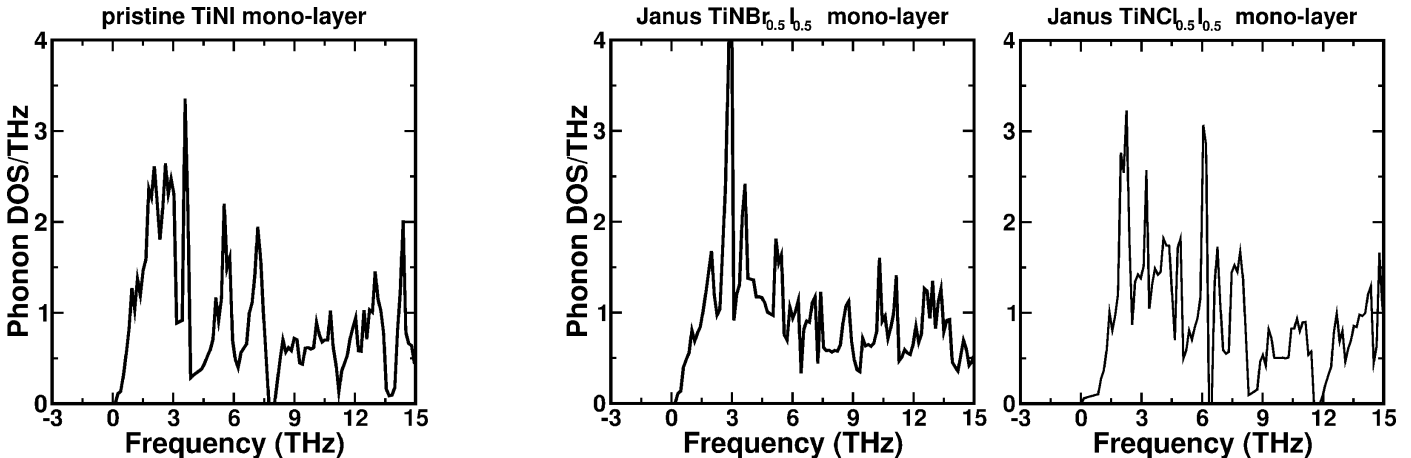


Figure 1: Phonon density of states, for the pristine TiNI and two Janus mono-layers calculated on their fully optimized structures.

The phonon DOS of the pristine TiNI mono-layer, indicates the dynamical stability for the pristine TiNI mono-layer, as seen previously. The two Janus mono-layers are also found to be dynamically stable as no imaginary frequency state was found.

Section S2

To ensure the thermal stability of the optimized structure for each studied mono-layer, *abinitio* molecular dynamic (MD) simulation was performed. The temperature was slowly increased upto 300 K using Noose-Hoover thermostat with a time step of 0.5 fs. Subsequently, the system was thermalized at this temperature for a duration of 20 ps. Figure 2 shows the variation of energy with the time step during the thermalization process, demonstrating the good thermal stability of the Janus structures at room temperature

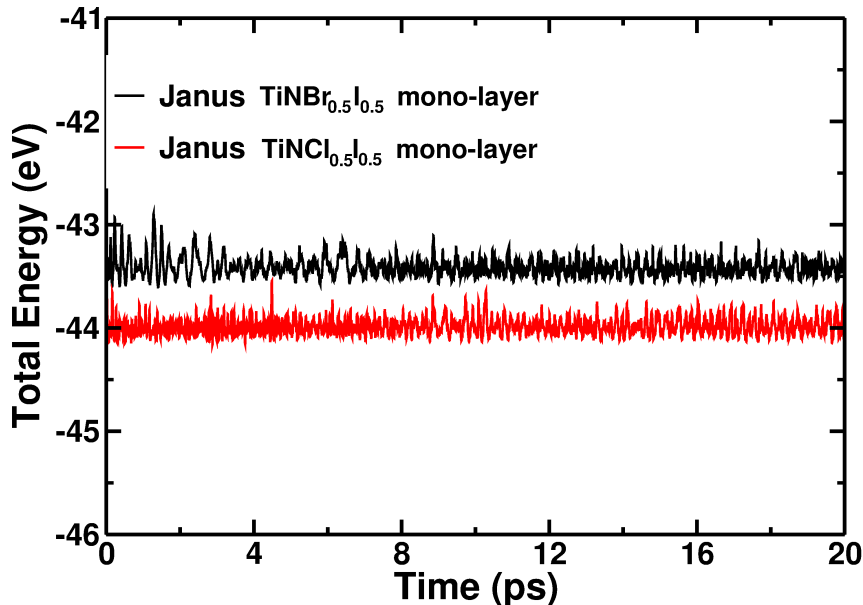


Figure 2: Molecular dynamics simulation at room temperature on the Janus structures for 20 ps, showing good thermal stability.

Section S3

As an alternative view of the projected band structure, we have also analyzed the important valance orbital projected density of states (PDOS) as shown in Fig. 3. It also clarifies that the valance state near the Fermi level is mainly contributed by I-5p and Ti-3d orbitals and the conduction state near the Fermi level is mainly contributed by Ti-3d states for each studied mono-layer. Furthermore, the contribution from Cl-3p or Br-4p states in the Janus

mono-layers are lower in energy compared to that of the I-5p states.

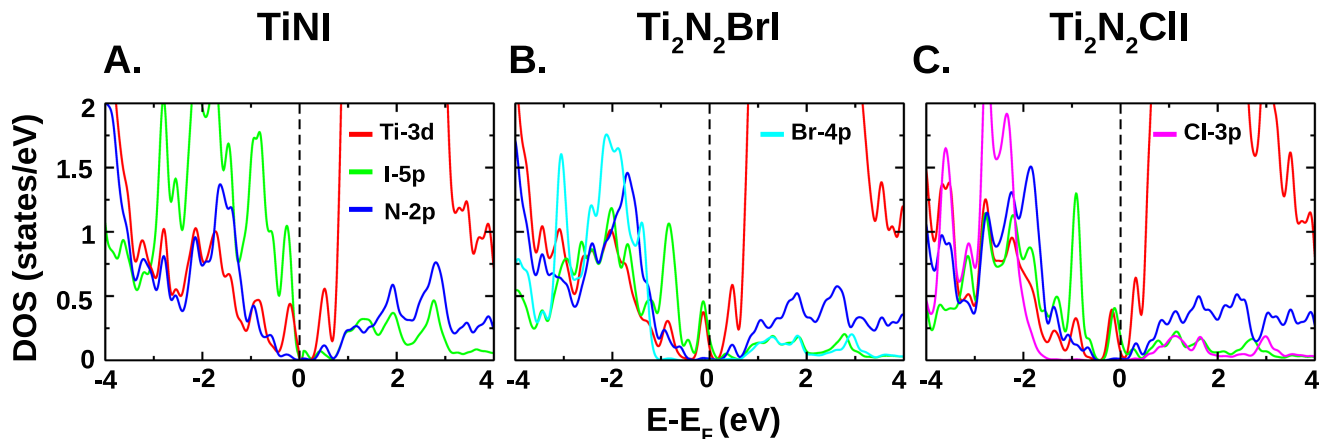


Figure 3: PBE+D3+SOC level computed valence orbital projected density of states of the constituting atomic species for the optimized structure of the studied mono-layer.

Section S4

To check the influence of choice of exchange-correlation, few of the calculations were repeated with HSE06 approximation for exchange-correlation. Although the unstrained structures were found to be narrow gap semiconducting with no band anti-crossing, therefore with trivial topology, the strained band structures were found to restore back the semi-metallic anti-crossing feature, along with non-trivial topology and large Rashba coefficient (c.f Fig. 4).

References

- (1) Togo, A., Tanaka, I. First principles phonon calculations in materials science. **2015** *Scr. Mater.*, *108*, 1-5.

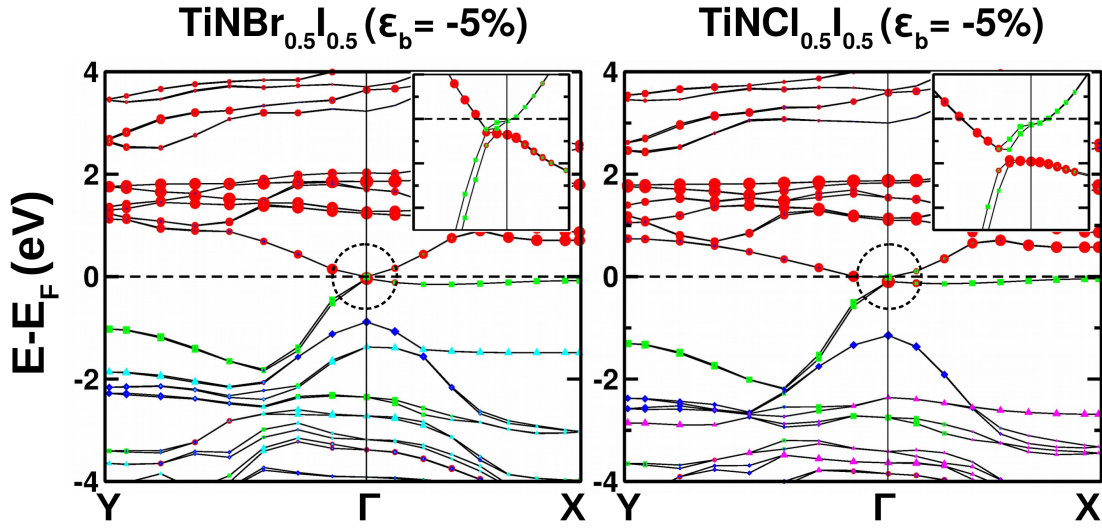


Figure 4: Band structures of the two uniaxially strained Janus monolayers for $\epsilon_b = -5\%$ calculated within HSE06+D3+SOC scheme of calculation. The band structure is projected onto Ti-3d (red), N-2p (blue), I-5p (green), Br-4p (cyan) and Cl-3p (magenta) orbital characters. The insets show the semi-metallic nature with anti-crossing points.